AIAA Aviation
16-20 June 2014, Atlanta, GA
19th AIAA International Space Planes and Hypersonic Systems and Technologies Conference

System Studies on Active Thermal Protection of a Hypersonic Suborbital Passenger Transport Vehicle

Tobias Schwanekamp[1] and Frank Meyer[2]
German Aerospace Center (DLR), Space Launcher Systems Analysis (SART) of the Institute of Space Systems, 28359 Bremen, Germany

Thomas Reimer[3] and Ivaylo Petkov[4]
German Aerospace Center (DLR), Space System Integration, Institute of Structures and Design, 70569 Stuttgart, Germany

Anke Tröltzsch[5] and Martin Siggel[6]
German Aerospace Center (DLR), Distributed Systems and Component Software, Simulation and Software Technology, 51147 Cologne, Germany

Aerodynamic heating is a critical design aspect for the development of reusable hypersonic transport and reentry vehicles. The reliability in terms of thermal resistance is one of the major driving factors with respect to the design margins, the mass balance and finally the total costs of a configuration. Potential designs of active cooling systems for critical regions such as the vehicle nose and leading edges are presented as well as preliminary approaches for their impact on the total mass. The visionary suborbital passenger transport concept SpaceLiner is taken as a reference vehicle for these studies. Covering the whole flight regime from subsonic to Mach numbers of more than 20, this vehicle creates high demands on the thermal protection system. Part of the work was performed within the DLR research project THERMAS.

Nomenclature

A	=	Area	m^2	$\dot{m}$	=	Mass flow	kg/s
α	=	Heat transfer coefficient	$W/(m^2K)$	p	=	Pressure	Pa
c_p	=	Specific heat capacity	J/(kgK)	Q	=	Heat	J
ε	=	Emissivity	-	$\dot{Q}$	=	Heat flow	W
h	=	Specific enthalpy	J/kg	$\dot{q}$	=	Heat flux	W/m^2
j_m	=	Mass flux	$kg/(m^2s)$	St	=	Stanton number	-
L/D	=	Lift-to-drag ratio	-	σ	=	Stefan-Boltzmann constant	$W/(m^2K^4)$
λ	=	Thermal conductivity	W/(mK)	T	=	Temperature	K, °C
M	=	Mach number	-	t	=	Time	s
m	=	Mass	kg	x,y	=	Coordinates	m

[1] Research Scientist, German Aerospace Center, Institute of Space Systems, Space Launcher System Analysis, Robert-Hooke-Str. 7, 28359 Bremen, Germany
[2] Student Assistant, German Aerospace Center, Institute of Space Systems, Space Launcher System Analysis, Robert-Hooke-Str. 7, 28359 Bremen, Germany.
[3] Research Scientist, German Aerospace Center, Institute of Structures and Design, Space System Integration, Pfaffenwaldring 38-40, 70569 Stuttgart, Germany.
[4] Research Scientist, German Aerospace Center, Institute of Structures and Design, Space System Integration, Pfaffenwaldring 38-40, 70569 Stuttgart, Germany.
[5] Research Scientist, German Aerospace Center, Simulation and Software Technology, Distributed Systems and Component Software, Linder Höhe 2b, 51147 Cologne, Germany
[6] Research Scientist, German Aerospace Center, Simulation and Software Technology, Distributed Systems and Component Software, Linder Höhe 2b, 51147 Cologne, Germany

I. Introduction

AEROTHERMAL problems are decisive for the design and the development of future reusable hypersonic reentry- and transport-concepts. Rapid deceleration of high enthalpy flows at the vehicle nose or leading edge induces very high stagnation temperatures whereas viscous flow phenomena such as shock/boundary layer interactions can cause local hot-spots downstream of the stagnation regions.

Different approaches can be followed to avoid structural damage due to high heat fluxes. A potential option, which is successfully practiced for reentry capsules, is the specific shaping of the vehicle shell. As the stagnation heat flux decreases with increasing nose or leading edge radius, a very simple solution is to strongly increase the bluntness of the stagnation regions and hence reduce the heat load peaks. Due to the very high wave drag during the hypersonic flight this option involves major shortcomings in the aerodynamic characteristics. Furthermore, today's thermal protections systems (TPS) for atmospheric re-entry are often based on ablative heat shields, which are certainly not the optimum choice in terms of the mass balance, the continuous shape change, the contamination of the boundary layer and the radiant heat of the ablation products. CMC (ceramic matrix composites) materials were found to be a promising alternative solution. However, the temperatures of these high temperature materials must stay below a certain maximum temperature to avoid active oxidation or erosion of the surface.

In contrast, future hypersonic transport concepts must be designed with maximum aerodynamic performance to be operationally efficient. This means a high lift-to-drag ratio (L/D) and therefore low drag which necessitates rather sharp and slender geometries with small nose and leading edge radii. Hence, the reliability in terms of thermal resistance is one of the major driving factors with respect to the design margins, the mass balance and finally the total costs. In addition to this, the rapid progresses in materials research, production and electronic engineering and simulation technology offer a novel potential for the design and manufacturing of efficient thermal protection systems. This is very important for the economy of future hypersonic transportation systems such as the visionary SpaceLiner, which was proposed by the DLR and is well described in Ref. 1 and Ref. 2. Figure 1 shows the artist's view of the SpaceLiner during the ascent, at booster separation and during the orbiter descent. Depending on the configuration or mission type, the maximum flight Mach numbers of the orbiter stage could reach 20 or even higher.

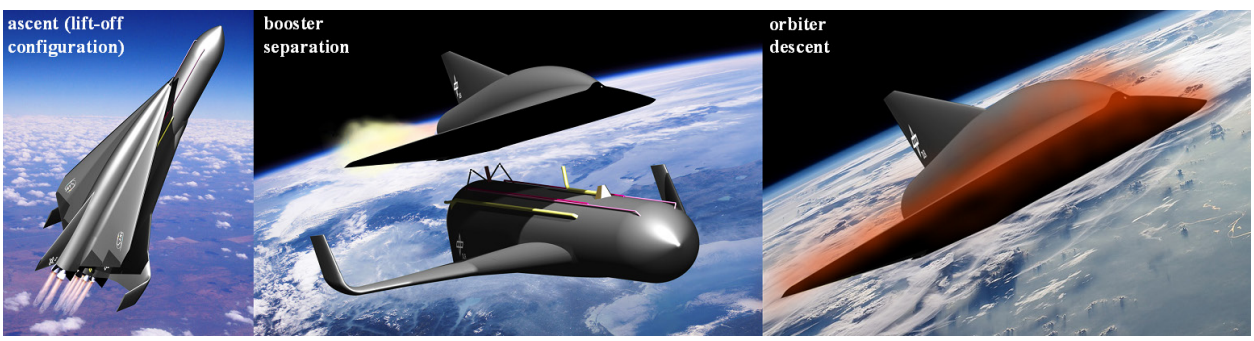

Figure 1. Artist's view of the SpaceLiner during flight.

Therefore intensive studies were conducted in order to optimize the outer shape of the SpaceLiner and to find a suitable trade-off between aerodynamic performance and thermal loads. Because the passenger stage covers the main part of the trajectory by gliding flight, an excellent L/D is required over a wide hypersonic Mach range, to achieve the travel destination. This requirement results in a relatively sharp nose and leading edge geometry which, in combination with the high Mach numbers, causes high heat fluxes and stagnation temperatures of more than 2500 K. Because these temperatures exceed the range of use of passive TPS materials, an efficient active system is required to reduce the maximum surface temperature. Additionally, the total mass must fulfill the systems requirements and economically justifiable effort for maintenance should allow for reusability of the components. To address these issues, the current study focuses on the investigation and the preliminary design of different active thermal protection systems.

Different cooling system architectures, materials and coolants have already been investigated in the past and this knowledge can be transferred to the SpaceLiner reference vehicle. Hence, after the specification of the system and the requirements an extensive literature research is conducted to get an overview of different cooling methods and to identify potential promising solutions for the SpaceLiner passenger stage. Each method has its specific advantages and drawbacks and must be assessed carefully with respect to the requirements of the SpaceLiner, which are mainly related to safety, reliability and low system mass. Therefore preliminary system designs of the most promising concepts are also elaborated in the framework of this study.

II. Methods and Tools

The analyses of the heat loads, the cooling efficiency and the system and coolant masses are conducted with DLR in-house tools and several engineering methods, which are suitable to get results with a reasonable computational effort and a sufficient amount of accuracy for the preliminary design phase.

For the simulation of hypersonic aero-/thermodynamics the surface inclination method HOTSOSE (HOT Second Order Shock Expansion method) was implemented at DLR to estimate the total aerodynamic coefficients as well as local surface parameters. Dependent on the particular geometry, Newtonian, modified Newtonian or Shock-Expansion Theory is applied to approximately determine the pressure distribution along the vehicle surface. In addition, HOTSOSE provides the option of approximately considering the influence of viscous effects either for ideal gas or in case of thermodynamic equilibrium flow assuming an isothermal or radiation adiabatic wall. The corresponding parameters such as radiation adiabatic wall temperature, heat transfer and skin friction coefficients are calculated by established engineering methods. Even if more complex aerodynamic phenomena such as shock-boundary layer interactions or interference drag cannot be reproduced by HOTSOSE, this method is well proven for preliminary design and suitable for a variety of vehicle shapes in hypersonic flow conditions[3,4].

To calculate aerodynamic characteristics with HOTSOSE the vehicle surface geometry has to be represented by a structured quadrilateral panel mesh. Therefore the very fast and efficient program GGH (Grid Generator for Hotsose) was implemented at DLR. Creating a text-based input file with the required geometric parameters enables GGH to automatically generate surface grids for a large variety of configurations within time frames of just a few seconds[5].

The DLR-SART program TOSCA_TS (Trajectory Optimization and Simulation of Conventional and Advanced space Transportation Systems, abbr. TOSCA) was implemented for the investigation of spacecraft ascent and descent trajectories. The user has to provide input data such as control parameters, aerodynamic characteristics of the vehicle (e.g. HOTSOSE output), structural and propellant masses, thrust as a function of the time, angle of attack and several optional parameters. With this input TOSCA is able to simulate and optimize flight trajectories and to calculate the correspondent trajectory data.

The evaluation of a very detailed and accurate mass model requires profound structural analyses as well as advanced dimensioning of systems and subsystems, aspects usually not applicable during the preliminary design process. Therefore the approximation tool STSM (Space Transportation Systems Mass) was developed at SART for zero and first level investigation of single and multiple stage configurations. It supports the early evaluation process and conveniently delivers data required at the pre-design phase, calculated via empirical correlations which reduce the amount of necessary input to a minimum. When entering first level analysis the results can be refined by including more elaborate information from additional tools. Hence the input-file is also designed to support a more accurate examination, if high quality data from additional tools are available. STSM can be utilized to detect the influence of the cooling systems on the full vehicle mass balance.

To be able to efficiently analyze and possibly optimize the overall system, the described preliminary design and simulation tools have been integrated as a process chain inside the Remote Component Environment (RCE)[6]. RCE is an open source distributed workflow-driven integration platform with a graphical user interface developed at the DLR and funded by the project THERMAS. RCE can be run in a distributed environment, where each simulation tool could be executed on a different computer so that it can remain at the place of the tool's experts. One of the main features of RCE is to be able to perform system analysis using either a design-of-experiments approach or by using the inbuilt optimization algorithms. In the case of the thermal protection analysis, this is a coupled optimization problem, where changes in the center-of-gravity caused by the structural sizing are feed back into the simulation of the aerodynamics (see Figure 2). To be able to solve such coupled optimization problems, multidisciplinary optimization (MDO) techniques are applied.

For validation purposes, the following simple optimization problem was formulated: The trajectory of the spacecraft is fixed and the configuration of the SpaceLiner is optimized for a sample flight point at an altitude of h=46 km and an approximate Mach number of M=19.8. The only varying design variable of the optimization problem is the nose radius of the fuselage. All other design parameters are fixed. The objective of the formulated optimization problem is to locate the nose design resulting in a minimal mass of the spacecraft (including liquids) subject to lower bounds on glide ratio and lift coefficient, and an upper bound on the pitching moment. Since most of the described integrated engineering tools do not provide derivatives of the objective function and constraint functions with respect to the design variables, only optimization algorithms that approximate, or do not need derivatives at all, can be applied. In the present case, the problem is solved using several publicly available software codes that are part of the Dakota optimizer suite[7], which is integrated into the RCE framework.

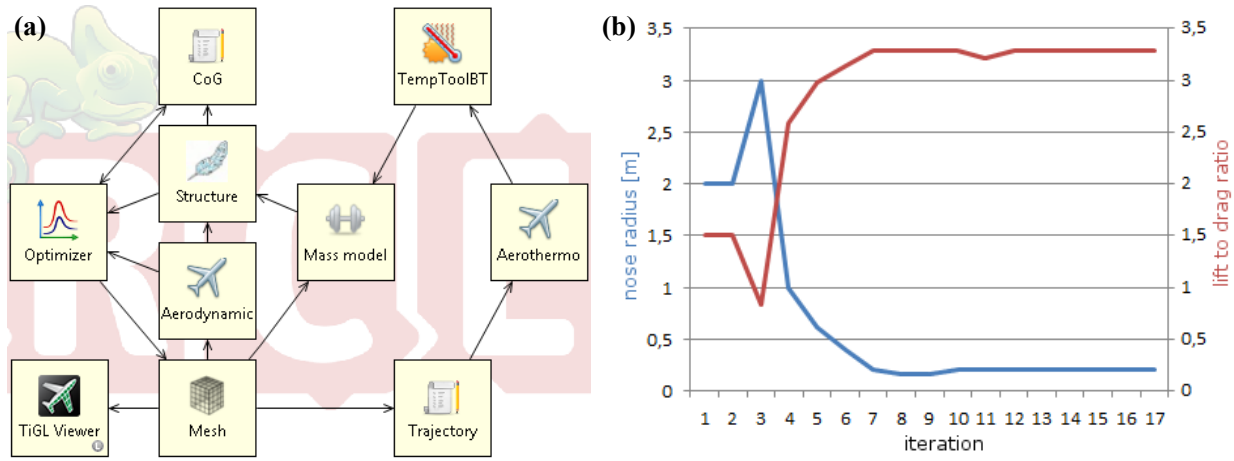

Figure 2. Optimization workflow within the RCE framework for thermal analysis (a). Example optimization of the nose radius using RCE (b). With decreasing nose radius, the L/D ratio improves.

III. System Specification and Requirements

For the design of a potential active cooling system the concept and mission requirements must be well defined. Figure 3 shows the altitude as a function of the Mach number for the reference mission from Australia to Europe. Due to the extent of validity of HOTSOSE, the hypersonic regime is considered for M>4, even if this is not an absolute limit. However, previous analyses have already shown that flight Mach numbers below M=4 do not have a major impact on the design of the active TPS anyway.

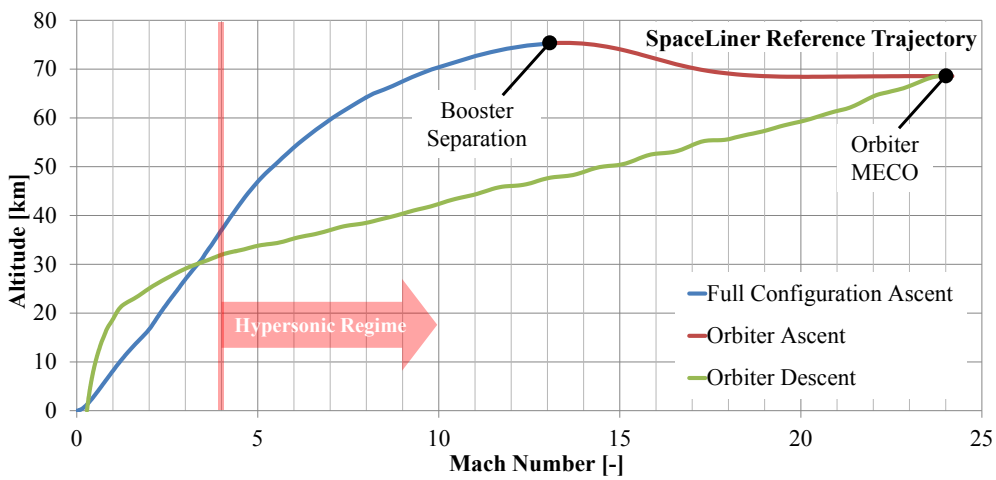

Figure 3. Altitude as a function of the Mach number for the SpaceLiner reference mission.

Figure 4 shows an estimation of the maximum occurring wall temperature T_{rad} and heat flux $\dot{q}_{rad}$ along the vehicle surface under the theoretical assumption of a radiation adiabatic wall (ε=0.83) for the full trajectory above Mach 4. The results were generated with HOTSOSE for hypersonic flow in thermodynamic equilibrium. The very high peak temperatures up to 2600 K shall be cooled down to a preferably constant cooling temperature, which is dependent on the chosen structure and wall material.

The heat flux, which is emitted by the surface through radiation, strongly depends on the local surface temperature T_W as given by the Stefan-Boltzmann law in Eq. (1).

$$\dot{q}_{rad} = \varepsilon \sigma T_W^4 \tag{1}$$

In case of a radiation adiabatic wall the total incoming heat flux is radiated away by the surface at the same time and no heat is transferred into the wall ($\dot{q}_W = 0$, Figure 5).

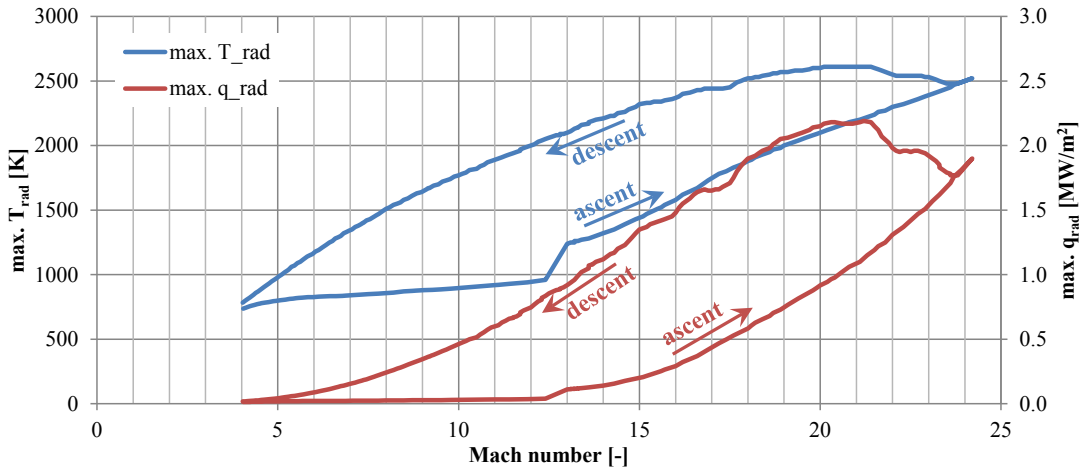

Figure 4. Maximum radiation adiabatic wall temperature and heat flux as a function of the Mach number for the SpaceLiner reference mission.

However, the very high radiation adiabatic temperatures detected for the SpaceLiner mission exceed the capacity of radiative TPS. Therefore additional active heat transport is required. If the wall temperature is actively cooled down below the radiation adiabatic temperature, the heat emitted by radiation decreases according to Eq. (1) whereas $\dot{q}_W$ rises. Hence, it must be noted that the heat flux $\dot{q}_W$ to be managed by the cooling system is strongly dependent on the wall temperature.

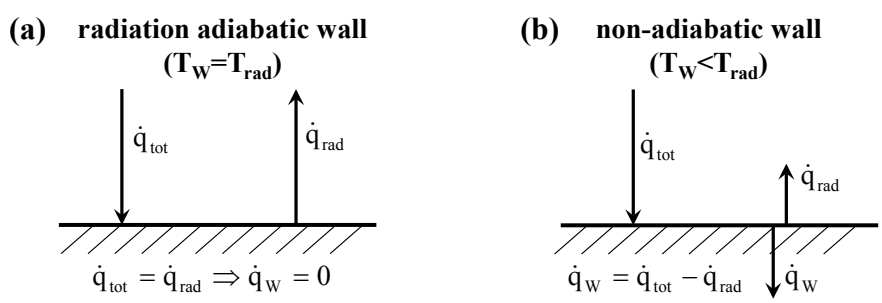

Figure 5. Surface heat flux for radiation adiabatic and non-adiabatic wall.

For the dimensioning of the SpaceLiner TPS two significant temperatures are defined. The first is the limiting temperature T_{lim}, which is derived from the upper temperature limit of the passive TPS material, selected for the less critical surface regions of the SpaceLiner in its current version. CMC (ceramic matrix composite) materials were found to be a promising solution. However, the temperatures of these materials must stay below a certain maximum temperature to avoid active oxidation or erosion of the surface. Based on previous projects such as THERMAS it was found that, for the C/C-SiC material which is investigated for the SpaceLiner, this critical temperature is approx. 1900 K. If the wall temperature exceeds T_{lim}, passive TPS cannot be used anymore and the particular zone must be actively cooled. In the present study the limiting temperature is set to T_{lim}=1850 K which includes a small margin of 50 K.

The second is the objective cooling temperature T_{obj} to which the surface in the critical regions shall be actively cooled down. To simplify the system analyses, T_{obj} is assumed to be kept constant by the active TPS during the full mission. The maximum acceptable value for T_{obj} is dependent on the properties of the wall and structure materials, which are selected for the active cooling system. The following requirements should be considered for the choice of a proper material:

- High thermal conductivity and transmittance
- High thermo-mechanical resistance and durability
- High resistance against corrosion and atmospheric conditions
- Preferably high operation temperature
- Low density, mass and cost

A main requirement concerning the wall and structure material is to quickly transfer the heat into the coolant. The heat transfer coefficient α defines the intensity of heat transfer across the interface between the structure and the coolant and is dependent on many factors such as the specific heat capacity, the density and the thermal conductivity of both the wall and coolant substance. Additional factors are for example the coolant velocity and flow characteristics as well as the interface geometry and the surface quality. Therefore high heat transfer rates can be realized either by the choice of appropriate materials and coolants or an optimal design of the heat exchanger geometry or, most suitable, a combination of both. Strong temperature gradients inside the material should be avoided due to thermo-mechanical stresses. This can be facilitated either by an adapted geometry design or by choosing a material with a high thermal conductivity respectively a high thermal transmittance. However, temperature gradients will always be present to a greater or lesser extent and, even if an isothermal wall is assumed for the simplified approach, the material temperature can vary over the time during the real mission. Therefore the material should feature a high thermo-mechanical resistance and durability. In addition the material should be resistant against potentially corrosive coolants and atmospheric conditions such as humidity. A high objective operation temperature has two advantages. On the one hand the fraction of heat emitted by radiation increases which, in turn, reduces the heat flux into the wall. On the other hand the required cooling power is reduced due to the decrease of the objective temperature difference $\Delta T=T_W-T_{obj}$, which must be compensated by the cooling system. From a systems point of view the total mass and with this the mass of each subcomponent is an important design factor. Heavy system masses create high demands on the propulsion and finally have negative effects on the overall costs. Hence, to reduce the overall mass it is advantageous to use materials with a low density. Besides the costs, which indirectly result from the mass, also the costs of the material itself should be preferably low.

T_{obj} does not only depend on the choice of the wall and structure material but also on the operational temperature range of the coolant, which is used for active heat transport within the system. The following requirements should be considered for the choice of a proper coolant:

- High heat transfer rates from the wall and structure material to the coolant
- High thermal conductivity and specific heat capacity
- Preferably high operation temperature
- Preferably easy and nonhazardous handling
- Low density, mass and cost

Finally, it should be mentioned that ablative heat shields shall not be applied for the SpaceLiner for two reasons. Firstly, this kind of TPS is in conflict with the demand for reusability of the full vehicle due to the need of ablator replacement after a strongly limited number of missions. Secondly, the crossrange capability and the aero-/thermodynamic performance would be negatively affected due to the continuous shape change, the contamination of the boundary layer and the radiant heat of the ablation products.

IV. Cooling Methods

Active cooling systems are already applied for some critical components of space transport systems, such as combustion chambers or engine nozzles. However, high temperature applications are not only limited to space transport and therefore a lot of information can be found about cooling methods in general. A literature research is conducted to get an overview of all these methods and to identify potential promising solutions for the SpaceLiner passenger stage in terms of system architectures, materials and coolants. This section focuses on the most interesting approaches, which are presented below.

A. Transpiration Cooling

For transpiration cooling, a gaseous or liquid coolant is injected through a porous or quasi-porous surface material into the external flow at the critical areas, where active thermal protection is required (Figure 6a). Thermal protection is achieved in two ways. On the one hand the coolant absorbs the heat from the porous material. On the other hand the boundary layer of the external flow near the wall is significantly affected by the evaporation of coolant, which can result in a substantial decrease of the convective heat transfer rate, the so called boundary layer heat blocking effect[8] (Figure 6b). Transpiration cooling methods are well described in the literature and a lot of reference data can be found. Ref. 9 gives a detailed overview of various cooling techniques and applications in aerospace and evaluates transpiration cooling with gaseous coolants such as air, nitrogen, hydrogen and helium in comparison to other methods. It is mentioned that the efficiency of transpiration systems with regard to heat flux and

time is, of course, limited by weight considerations, including the necessary tankage, pressurization and distribution hardware. But, it is stated that transpiration systems appear to become superior to other absorptive systems at long operation times and extreme heat fluxes.

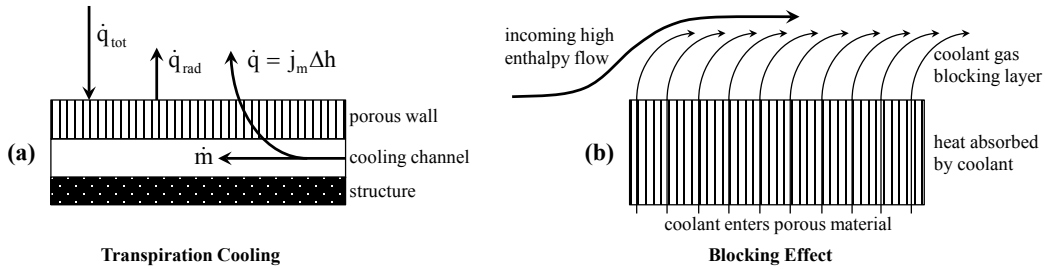

Figure 6. Transpiration cooling and blocking effect.

Similar studies have been performed by Gomez[10,11] on a rather systems oriented level. In particular, design studies on an active transpiration cooling system for the leading edge of a potential Space Shuttle successor were conducted, considering gaseous air, nitrogen, hydrogen and helium but also liquid coolants, which vaporize at the wall interface. For gaseous coolants it was observed that the use of light molecular weight gases provides the most effective cooling designs, e.g. helium systems were found to be two to three times lighter than oxygen systems. Coolants which flow into the porous matrix in the liquid phase and make use of the vaporization enthalpy of the liquid-vapor phase change were found to be many times more effective than gaseous coolants.

Following up this approach, an innovative method of transpiration cooling using liquid water as a coolant was investigated for the SpaceLiner at the DLR arc-heated wind tunnels in Cologne[12,13] (Figure 7), resulting in a first estimation of the required cooling water mass for the full SpaceLiner mission. A very high cooling efficiency of water was experimentally proven. Stagnation point temperatures of more than 2000 K were cooled down by about 1500 K with very low coolant mass flows. In comparison it was shown that even a five times higher nitrogen gas mass flow could only achieve a temperature drop of 600 K. In addition to the tests, simulations were conducted utilizing the HOTSOSE code. Compared to the experiments an approx. 30% higher required water mass flow was calculated, which was attributed to the blocking effect that could not be modeled by HOTSOSE. Referring to these results, the HOTSOSE simulations are a rather conservative approach.

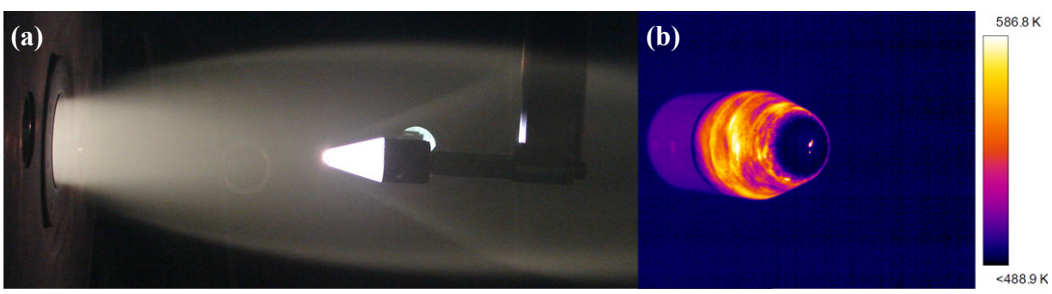

Figure 7. Test in L2K arc heated wind tunnel (a) and cooled model temperature distribution (b)[14,15].

However, besides the evident advantages of transpiration cooling with liquids, fundamental issues and challenges have already been identified which, in the worst case, might put the whole application of the concept into question. First, it was shown not only for vaporization of liquid coolants but also for gaseous coolants that injecting a flow into the boundary layer can strongly affect the laminar-turbulent transition downwards of the cooled region. Dependent on the particular state and condition of the flow this can cause local hot spots downstream the cooled surface. This is shown in Figure 8 for a sample surface which was partially cooled with gaseous helium[14]. The temperatures and Stanton numbers at the hot spot can even exceed the values without any cooling. As the appearance and location of these hot spots is extremely difficult to predict for non-steady real flight conditions, it might be a severe problem for the SpaceLiner. In addition the triggering of laminar-turbulent transition can also have a negative influence on the aerodynamic performance (L/D).

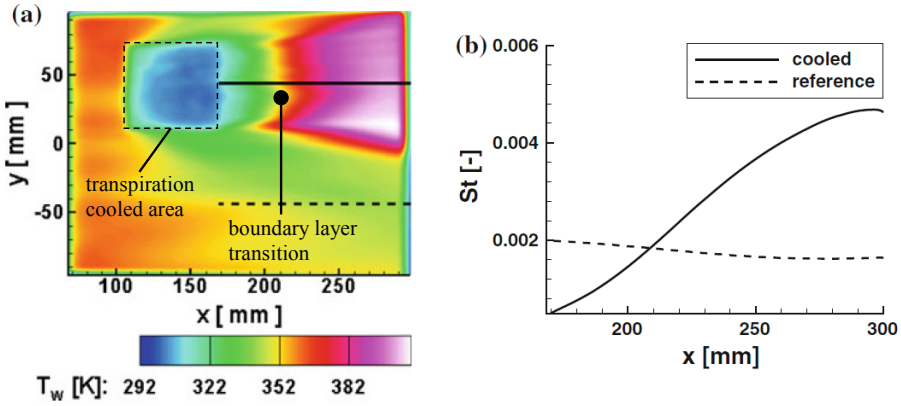

Figure 8. Measured temperature (a) distribution and Stanton number profiles (b) for the test with helium as coolant[14].

Another issue which became obvious during the wind tunnel tests in Ref. 12 is particularly related to the use of liquid water. Dependent on the porous material, the exact adjustment of the coolant mass flows through the surface was found to be very complicated, especially for CMC materials. The coolant mass flow was either too low or too high. This means that the objective cooling temperature, which is assumed to be achieved by active cooling within the present studies, might not be achievable within the practical application. For low mass flows the water already started to boil within the coolant chamber before entering the porous material, implying the risk of damaging the test model. For high mass flows the model surface was covered by liquid water, cooling down the surface far below the objective temperature. Actually, besides the performance losses, this would not really be critical for the system.

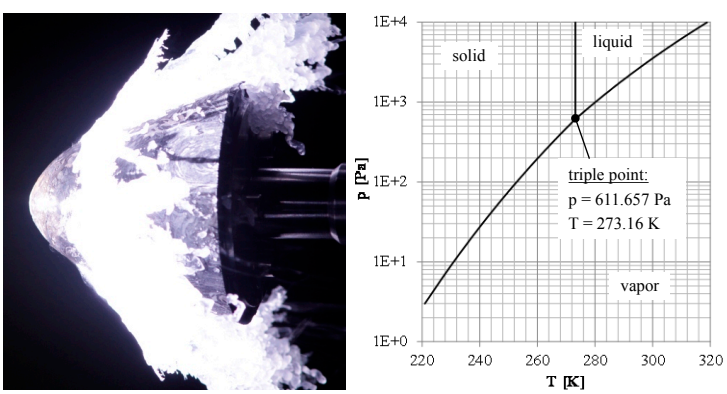

Figure 9. Ice formation for transpiration cooling with liquid water due to low pressures[12] and phase diagram of water.

However, an interesting effect occurred during the tests. As pressure in the wind tunnel was already very low and the gradients in the model surface caused even further pressure drops in the passing surface flow, the local surface pressure fell below the pressure of the triple point of water. In combination with the high water mass flow and the high cooling rates, this caused the formation of an ice shroud (Figure 9). The preliminary analyses of the SpaceLiner trajectory have shown that this effect might also occur during the real mission. This would result in drastic losses of safety and aerodynamic performance.

Modeling these effects numerically is an extremely complex task and cannot be performed within the present studies. However the specific issues related to transpiration cooling must be taken into consideration for the evaluation of this method for the SpaceLiner.

B. Convective Cooling

Convective or regenerative cooling methods utilize the forced convection of liquid or gaseous coolants to carry away the heat from thermally critical surface regions and hot spots. The coolant flows through small channels below or within the wall material, either turbulent or laminar, depending on the Reynolds number and the inlet conditions (Figure 10). Convective and regenerative cooling methods are extensively described in the literature and a lot of reference data can be found.

McConarthy[15] gives an extensive evaluation of different cooling techniques for a Mach 6 cruise vehicle concept. According to that it can be distinguished between direct and indirect convective cooling systems. For direct systems the coolant passes the thermally critical area and is then carried away to other areas of the vehicle where it may be either dumped or consumed or the heat is radiated away or soaked in a heat sink and the coolant is reused again in a closed cycle. For indirect systems a closed heat transport loop transfers heat from the areas to be cooled to the heat exchangers, where the heat is transferred to another coolant in a second loop, which might either carry the heat away

in a closed or an open cycle then. The complexity of those systems is, of course, higher than for direct systems but on the other side indirect systems offer a greater flexibility in terms of coolant choice, operating temperature levels and insensitivity to gravitational effects. Since the weight of the basic structural component is usually greater than that of the cooling system hardware, the most desirable operating temperature levels are those which permit the use of low density structural alloys such as aluminum or titanium.

Direct regenerative cooling is also used to protect the nozzles of liquid rocket engines from the high thermal loads. This technique is, for instance, applied to expander cycle rocket engines such as the Vinci rocket engine, which is currently under development by ESA to power the new upper stage of Ariane 5. Therefore the propellant is ducted through small passages around the nozzle wall before entering the combustion chamber. The use of rocket propellants such as liquid or gaseous hydrogen or oxygen as coolants is also advantageous since these coolants are available anyway and no additional external storage must be provided. However, leakage might be an issue to consider in terms of safety for the use of hydrogen as a coolant in the civil transport sector. In particular, leakage might be caused by thermo mechanical stresses and fatigue of in the wall material, because one side is exposed to the high enthalpy flow, whereas the other side is in contact with the relatively cold coolant fluid, which can cause strong thermal gradients in the material[16].

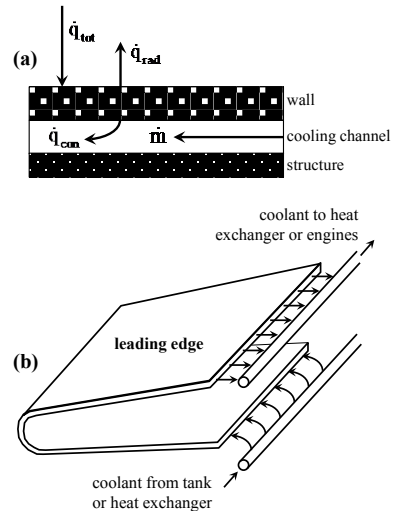

Figure 10. Convective cooling, principle (a) and schematic application to a leading edge (b).

Convective cooling can either be performed by gaseous or liquid coolants. Dependent on the coolant, the exploitation of the vaporization enthalpy is not recommended, because the two-phase flows within the cooling channels are complicated to handle. This is, for instance, the case for water. For the vapor phase the heat transfer from the wall to the coolant is completely different than for the liquid phase. As there are large uncertainties in the location of the boiling position within the cooling channel, the heat transfer characteristics of such a system would be very difficult to control. Glass[17] presented a system, composed of heat pipes with lithium as a coolant and an optional second cooling loop with hydrogen as a coolant (indirect system). The previously mentioned problem of could be solved by a system like this. However, due to the preliminary character of the present studies, either fully gaseous or fully liquid coolants are considered for convective cooling. The design and operational aspects such as the mass flow control of convective systems are less complex than for the transpiration cooling system.

C. Spray Cooling

Actually, spray cooling can be considered as a special type of convective cooling, which systematically exploits the high vaporization enthalpy of liquid coolants such as water. The previously mentioned problem of undefined boiling and heat transfer characteristics is less critical due to the application of a very thin coolant film on the inner material surface, which is continuously vaporized and replaced by a defined jet spray mass flow coming from the cooling spray nozzle (Figure 11). This method was already described for the leading edges of a Mach 6 vehicle[15] but not yet practically applied in the aerospace sector. However, it is widely used within the process metallurgy due to the capability of generating very accurate and well defined heat transfer rates[18]. Of course, the issue with thermal stresses and fatigue, which is evident for all convective cooling methods, might also occur for spray cooling. But, due to the very precise controllability, this problem seems less critical here.

Ref. 18 gives a method to almost completely avoid the so-called Leidenfrost effect by mixing the liquid coolant with a carrier gas mass flow (Figure 13). The Leidenfrost effect describes the phenomenon in which a liquid, in near contact with a surface significantly hotter than the liquid's vaporization temperature, produces an insulating vapor layer, which keeps that liquid from boiling rapidly. The effect which can also occur for convective cooling with liquid-vapor phase change has a strong impact on the heat transfer rates. This is illustrated in Figure 12 for water with the initial temperature T_{H2O} and the wall temperature T_W. The gradient for evaporation cooling is approx. 30 times larger than for film boiling. It was shown that for evaporation cooling, no continuously wetted water film is built up on the hot surface. If the water mass flow is further increased and a certain maximum mass flow density impinging on the surface is exceeded, a water film is formed, which in turn creates an underlying vapor film, if the wall temperature is higher than the Leidenfrost temperature.

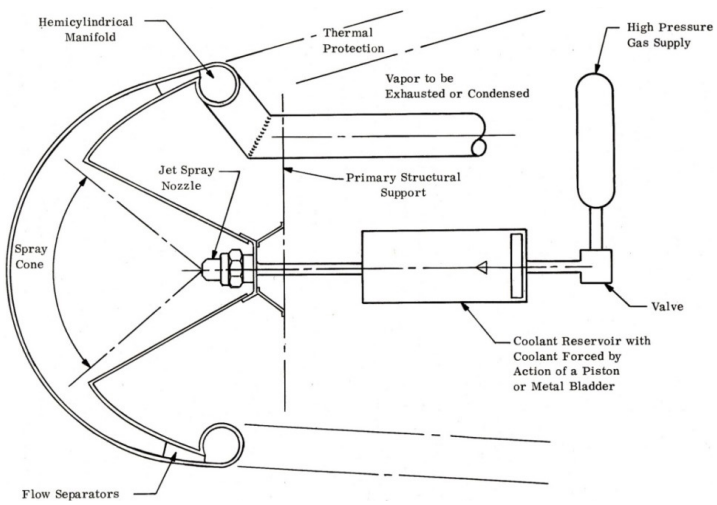

Figure 11. Spray cooling[15].

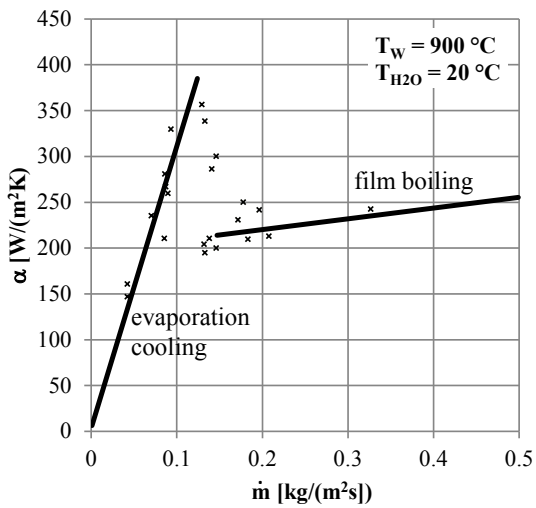

Figure 12. Evaporation cooling and film boiling[18].

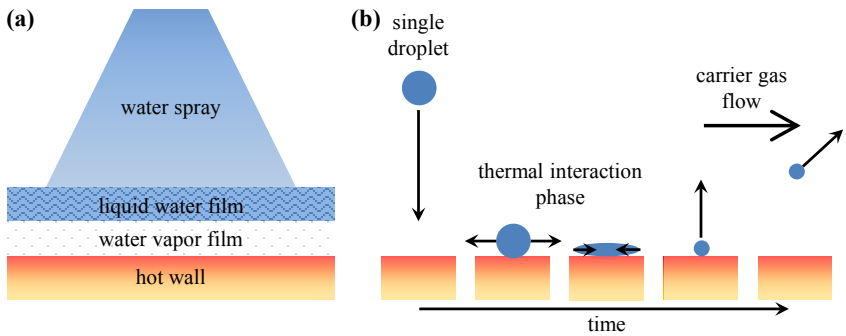

Figure 13. Schematic illustration of spray cooling with liquid water (a) and liquid water with carrier gas mass flow (b)[18].

D. Heat Conductive Fibers

As part of the THERMAS project the improvement of the thermal and mechanical properties of the C/C-SiC ceramic matrix composite material is pursued. The goal is to transfer the advantageous properties of pitch based carbon fibers, such as high thermal conductivity and high stiffness to the ceramic composite material C/C-SiC shown in Figure 14. Based on the high thermal conductivities of pitch based carbon fibers of up to 1000 W/(mK) compared to 15 W/(mK) for the currently used PAN fibers it was assumed that a CMC material with a thermal conductivity in the range of aluminum could be produced. FE modelling of the CMC microstructure and numerical analysis of the thermal conductivity were performed and the generated data used to preliminary estimate the passive cooling capability of the material.

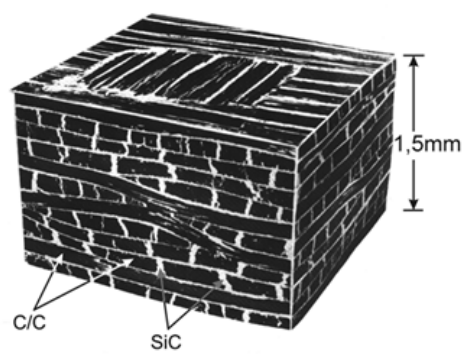

Figure 14. Microstructure of C/C-SiC ceramic matrix composite.

The pitch carbon C/C-SiC material relies on high effective thermal conductivity (due to the graphitic nature of the fibers) to move heat from an area of intense, localized heat (leading edge or nose cap area) to cooler locations where it can be effectively rejected from the vehicle's surface or internally stored (e.g. by heating fuel). This passive cooling concept can be applied for temperatures of up to 1650°C. Hence, for the SpaceLiner this concept could only be applied in combination with active cooling within a hybrid system. A detailed mass analysis is therefore not conducted in the present paper but instead the results of the studies within the THERMAS project are shown.

V. Concept Development and Evaluation

For the preliminary design of active cooling concepts it is not only important to know the maximum occurring heat fluxes and temperatures along the flight trajectory but also the total heat flow, integrated along the critical zones of the vehicle surface for each time step of the trajectory. The total heat to be absorbed by the coolant strongly depends on the temperatures T_{lim} and T_{obj}, which were mentioned in section III. T_{lim} has a direct impact on the size of the critical surface region A_{crit}, where T_{lim} is exceeded during the mission. A_{crit} significantly grows with decreasing T_{lim} (Figure 15). The difference between the objective cooling temperature T_{obj} and the radiation adiabatic temperature T_{rad}, which would occur without any cooling has an impact on the fraction of the local heat flux, which must be carried away by the coolant. It is obvious that the heat flux to be absorbed and thereby the required coolant mass flux will increase, if the surface should be cooled down from higher values of T_{rad} to lower values of T_{obj}. The simulations will be performed with a limiting temperature of T_{lim}=1850 K, as stated in section III, and for three different objective temperatures 500 K, 1000 K and 1500 K.

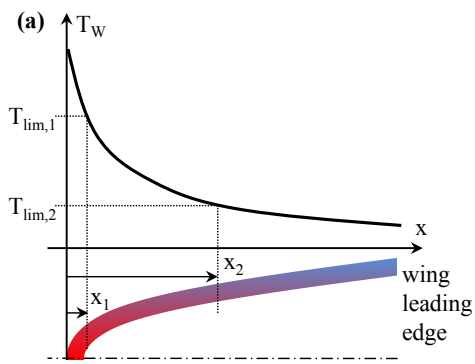

(b)

T_{lim} [K]	A_{crit} [m^2]
1500	76.47
1600	46.35
1700	29.64
1800	21.36
1900	16.25

Figure 15. Qualitative temperature distribution and limiting temperature regions along the x-direction of a leading edge (a). Total critical surface area A_{crit} for the full SpaceLiner mission and different T_{lim} (b).

For the recent SpaceLiner reference mission the limiting temperature of 1850 K results in a critical area A_{crit}=16.36 m^2 which is located at the wing leading edges and the vehicle nose (Figure 16). For the remaining surface a reusable passive TPS will be sufficient. This was already dimensioned for the SpaceLiner orbiter[19] and is not part of the present study. It must be noted that the active TPS should not be designed to carry any mechanical loads.

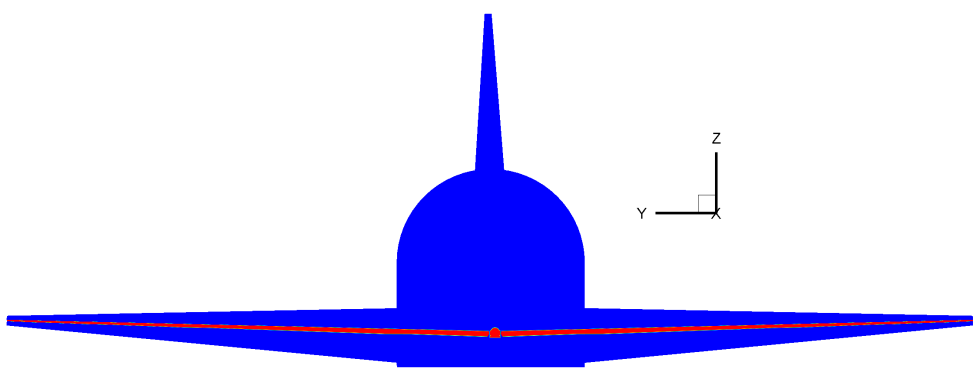

Figure 16. Critical surface area (red) at the nose and leading edges, where T_{lim}=1850 K is exceeded during the mission

The heat, which must be absorbed by the cooling system, can approximately be estimated by running HOTSOSE twice for every flight point of the mission trajectory. The simulation is conducted once under the assumption of radiation adiabatic equilibrium to identify the critical surface regions which require active cooling. Then the simulation is conducted a second time within the critical regions, assuming an isothermal wall with the constant temperature T_{obj}. The heat fluxes calculated for the isothermal case are to be absorbed by the cooling system to keep the temperature T_{obj} on a constant level. The heat fluxes are then firstly integrated along the vehicle surface and

secondly along the full flight trajectory to achieve the total heat to be absorbed. Figure 17 shows the heat flow $\dot{Q}_{crit}$ in the critical regions as a function of the flight time for the three different objective temperatures and the integrated total heat within the critical areas for the full mission. It must be noted that the rapid drop in heat flow between approx. 440 s < t < 460 s is caused by a very high angle of attack manoeuver after MECO, which was found to be necessary for an optimum reentry flight.

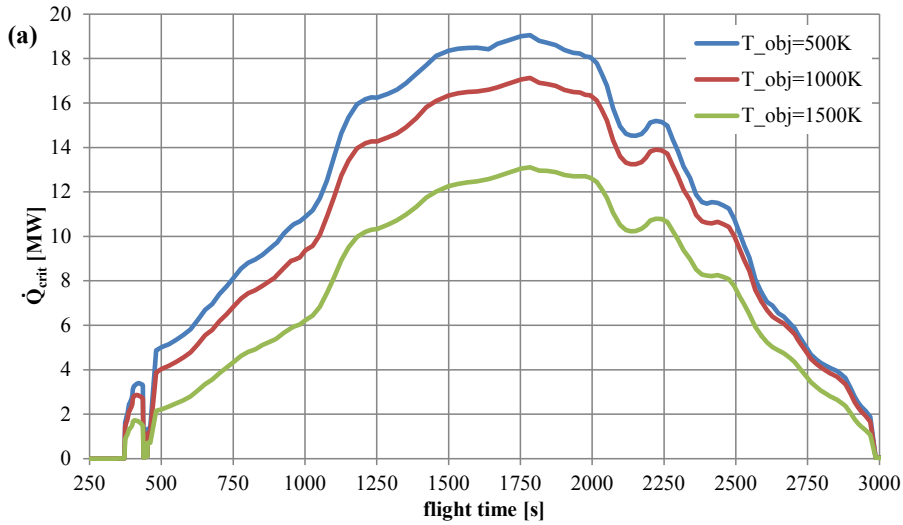

(b)

T_{obj} [K]	Total Heat [MJ]
500	31018.5
1000	27682.5
1500	20424.4

Figure 17. Heat flow integrated along the critical vehicle surface areas as a function of the flight time (a) and total heat in the critical surface areas integrated along the full mission time (b).

The total heat Q_{tot} to be absorbed during the mission has a direct impact on the required mass of the coolant. As the studies conducted within the present section are of rather preliminary character, an ideal heat transfer will be assumed to simplify the investigations. This means that all the heat, which must be carried away by the cooling system, will be fully absorbed by the coolant. Even if this is an optimistic assumption in comparison to the reality it is still suitable for a qualitative evaluation and comparison of the different system approaches.

For the estimation of the total systems masses the required coolant mass is considered as well as the preliminary mass breakdown of the main subcomponents. Detailed information about the mass determination can be found in Ref. 20. The main results are given in the following sections for each system approach. It must be noted, that the mass estimations are based on very simple approximations and must be iteratively refined in future studies.

A. Transpiration Cooling

An active transpiration system with liquid water as a coolant was designed for the SpaceLiner (Figure 18). The system is designed symmetrically for redundancy reasons and also due to the available space in the intersection between the fuselage and the wings. To enable better mass flow control, both leading edges are separated into eight separated coolant chambers. Each chamber has a constant perimetric length of 1.2 m. The porous C/C-SiC layer thickness is 10 mm.

The mass of the single components was estimated by simple engineering methods, considering the required water pressure and mass flow which is required for cooling down the surface to a constant temperature T_{obj}. Because the water evaporates through the wall into the ambient conditions, the external pressure must be considered to determine the vaporization enthalpy of water. For the estimation of the water mass only the vaporization enthalpy is considered whereas the enthalpy due to temperature change within one phase is neglected. Dependent on the objective cooling temperature, different water mass flows and total required masses were calculated (Figure 19). For the design of the tanks the total water mass is, of course, a dimensioning factor. For the design of the lines and the distribution system, the maximum mass flow rates at the particular locations must be considered for the most critical point of the trajectory. A detailed description of the applied correlations and equations for the dimensioning of the coolant tank and line system is given in Ref. 20. The most important results for the system masses are given in Table 1 for the three different objective cooling temperatures. As for most of the SpaceLiner subsystem masses in the preliminary design phase a margin (20%) is included within the given values. It can be noted that the tanks are relatively light weight because of the low internal pressure of 100kPa due to the external pump. The percentage of

the active cooling system mass related to the total passenger stage empty mass (incl. margins) is given in brackets in Table 1.

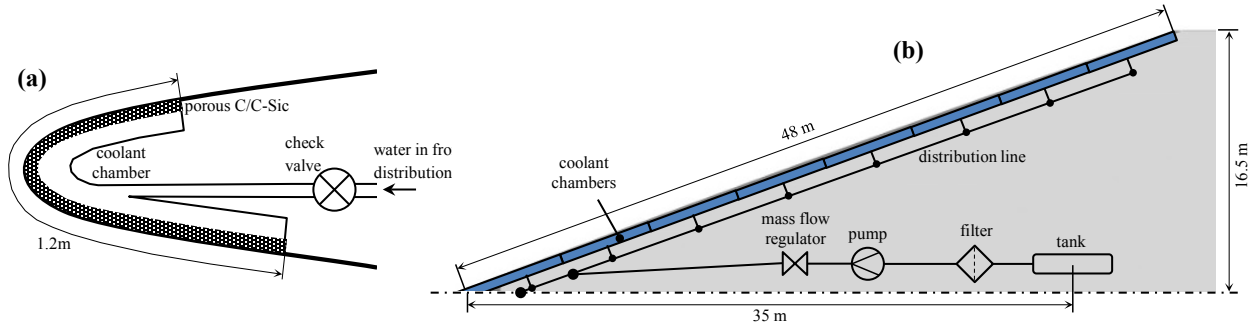

Figure 18. Potential preliminary design of active transpiration cooling system with liquid water for the SpaceLiner nose and leading edge, profile cross section (a) and plan view (b).

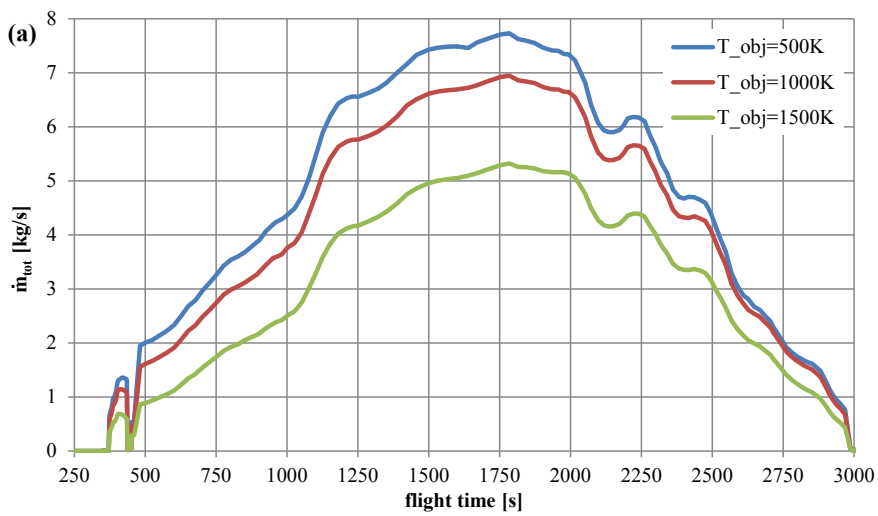

(b)

T_{obj} [K]	Total Water Mass [kg]
500	12562
1000	11213
1500	8275

Figure 19. Water mass flow integrated along the critical vehicle surface areas as a function of the flight time (a) and total water mass integrated along the full mission time (b).

component	m [kg] (T_{obj}=500K)	m [kg] (T_{obj}=1000K)	m [kg] (T_{obj}=1500K)
pipes	146	146	146
tanks	320	295	241
pumps	310	280	212
valves	14	14	14
mass flow regulators	10	10	10
filters	12	12	12
porous wall (C/C-SiC)	880	880	880
coolant	14890	13274	9791
total	**16582 (10.4%)**	**14911 (9.3%)**	**11306 (7.1%)**

Table 1. Preliminary mass break down for the transpiration cooling system with liquid water.

Due to the potential problem of ice formation, alternative gaseous coolants might be an option. As no phase change happens, only the enthalpy due to temperature increase of the coolant gas can be used then. Therefore the required coolant masses strongly depend on the specific heat capacity and the difference ΔT of the initial and final

temperature of the coolant. The initial temperature T_{in} can be well defined by the tank and distribution line conditions and is set to a fixed value of 300 K here, which is close to the SpaceLiner propellant tank pressurization gas temperature and should easily be achievable. In a first guess it is assumed that the final temperature T_{fin} of the gas after passing through the porous wall material is approximately equal to the objective cooling temperature of the wall. For the calculation of the gas mass, the specific heat capacity at standard conditions is taken into account. Table 2 shows an overview of different coolant masses calculated via Eq. (2).

$$m_{tot} = \frac{Q_{tot}}{c_p \Delta T} \tag{2}$$

Even if this is a strongly simplified approach the general tendencies become very clear here. From a systems point of view it is obvious that only hydrogen and helium fulfill the mass requirements of the configuration. The advantages of hydrogen are of course the very high heat capacity and the availability due to the propulsion system. No additional tanks would be required to store the hydrogen. Therefore the potential ΔT could even be increased because the hydrogen is stored under cryogenic conditions in the propellant tank. But, for the use in transpiration cooling at high temperatures in oxygen rich atmosphere hydrogen can obviously not be recommended due to the risk of combustion. Therefore helium would be the only promising gaseous alternative. Disadvantages are the need for an additional system and the relatively high costs of helium.

coolant	c_p [kJ/(kg K)]	m_{tot} [kg] (ΔT=200K)	m_{tot} [kg] (ΔT=700K)	m_{tot} [kg] (ΔT=1200K)
hydrogen	14.304	10843	3098	1807
helium	5.193	29866	8533	4978
nitrogen	1.04	149127	42607	24854
oxygen	0.92	168579	48165	28096

Table 2. Comparison of different gaseous coolant masses.

B. Convective Cooling

Figure 20 shows the schema of a potential preliminary design of a convective cooling system for the SpaceLiner nose and leading edge. Analog to the transpiration cooling system, this system is also designed symmetrically for redundancy and space reasons. The cooling channels are distributed directly at the back of the wall material adjacently to each other with the same perimetric length of 1.2 m than for the transpiration system chambers. As there is no porous material which might be choked by particles in the coolant, a filter unit is not considered to be necessary here. Within the current approach the coolant is dumped via the collector pipe after passing the cooling channels. It could also be an option to further use the heated coolant for power generation or attitude control.

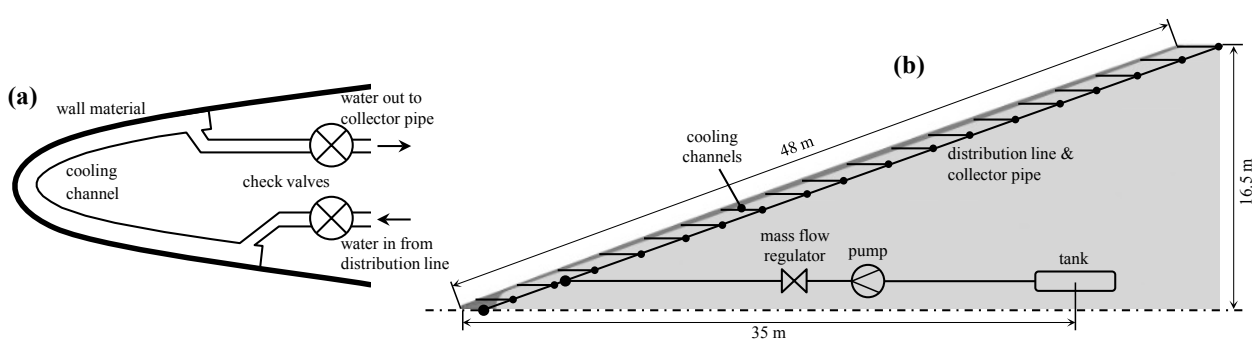

Figure 20. Potential preliminary design of convective cooling system for the SpaceLiner nose and leading edge, profile cross section (a) and plan view (b).

As the convective cooling system is less restricted with respect to potential coolants compared to the transpiration cooling, different coolants were taken into account during the analyses. A maximum pressure of p_{max}=100 kPa shall be kept in the cooling channels by the pressure check valves. This pressure is also considered for the design of the system and the calculation of the coolant masses.

Considering the vaporization of liquid water in a first guess, approximately the same masses than for transpiration cooling would be necessary. The low density and thermal expansion makes C/C-SiC also a suitable material for the wall and cooling channel design. Furthermore it is advantageous because the high temperature material allows for higher objective cooling temperatures and therefore a decrease of coolant mass. The porous C/C-SiC must be replaced by non-porous C/C-SiC material. The main results for convective cooling with liquid water are given in Table 3.

component	m [kg] (T_{obj}=500K)	m [kg] (T_{obj}=1000K)	m [kg] (T_{obj}=1500K)
pipes	1010	1010	1010
tanks	320	295	241
pumps	310	280	212
valves	1100	1100	1100
mass flow regulators	10	10	10
coolant	14890	13274	9791
total	**17640 (11.0%)**	**15969 (10.0%)**	**12364 (7.7%)**

Table 3. Preliminary mass break down for the convective cooling system with liquid water.

The design envisages a total number of 1500 cooling channels with a cross section of 10 mm (height) times 20 mm (width) distributed along the leading edges and nose (Figure 21). The wall material mass is already included in the cooling channel (pipe) mass. More detailed information about the design process can be found in Ref. 20.

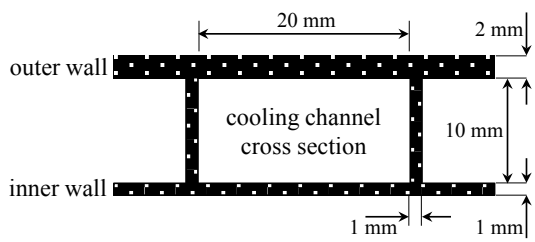

Figure 21. Cross section geometry of the convective cooling channel.

The total system masses are slightly higher than for the transpiration cooling with liquid water. This is mainly caused by the very high numbers of cooling channels and the respective complex distribution valve system. However, if two or more cooling channels would be combined into a group with only one valve the respective mass fraction could be saved. Therefore it can be stated that the overall masses of transpiration and convective cooling with liquid water are within the same order of magnitude.

For the convective cooling system the use of gaseous hydrogen is assessed to be less critical than for the transpiration cooling. If the system could be designed absolutely safe against leakage, hydrogen could bring enormous mass savings due to its very high specific heat capacity and also because there would be no need for an additional tank. Another advantage is that the hydrogen in the propellant tank is stored in the cryogenic state with a temperature of around 20 K, which increases the temperature range that can be used for the cooling. Due to the heat input in the pipes an effective hydrogen gas temperature of 50 K is assumed for entering the cooling system. Considering these new values Table 3 can be modified as shown below (Table 4) incl. 20% margins.

component	m [kg] (ΔT=450K)	m [kg] (ΔT =950K)	m [kg] (ΔT=1450K)
pipes	1010	1010	1010
pumps	310	280	212
valves	1100	1100	1100
mass flow regulators	10	10	10
coolant	5783	2444	1182
total	**8213 (5.1%)**	**4844 (3.0%)**	**3514 (2.2%)**

Table 4. Preliminary mass break down for the convective cooling system with gaseous hydrogen.

It must be noted that the additional mass due to the increase of the propellant tanks is not yet included. However, as the coolant mass is the main impact factor on the total mass of the cooling system, the mass savings with using

hydrogen are very high compared to water. Another question to be answered within future studies is related to the differences in the heat transfer coefficient between liquid water and gaseous hydrogen. As the heat transfer from the wall into the coolant is lower for gaseous coolants, a more complex heat exchanger geometry may be required, which brings additional mass to the system.

A third option was analyzed using lithium as a coolant. The advantages of lithium are the very low mass and the extremely high vaporization enthalpy of approx. 21000 kJ/kg. The boiling temperature of Lithium at 101.3 kPa is T_{vap}=1615.15 K. Therefore a high temperature material such as C/C-SiC is definitely required. For an objective cooling temperature of 1615.15 K a total heat during the full mission in the critical regions is calculated by 17751.8 MJ, which is accordant to the vaporization enthalpy of 846 kg Lithium. However, there are many reasons to not recommend the use of Lithium in an open convective cooling cycle such as the high costs and the melting point of 453.7 K, which makes the handling quite difficult. Therefore the use in an indirect system seems to be more attractive. The heat pipes are suitable for managing the extreme heat load peaks in the stagnation region. As heat pipes are closed systems, the heat must be carried away by a second cooling loop. A hybrid system like this will be investigated in future analyses.

The same circumstances are present for the use of heat conductive fibers. These fibers are suitable to damp the heat load peaks in the stagnation regions by transporting the heat downwards the stagnation regions. Therefore the question arises where to get rid of the heat. A second cooling loop would be required also in this case.

C. Spray Cooling

A first and rough approach for active spray cooling with liquid water was considered within the present studies (Figure 22). The principal arrangement of the components is similar to the transpiration cooling but no porous wall material is implemented and a large number of cooling units (nozzle array, valve and implementation structure) is required. Three nozzles are planned to be implemented per array. The span-wise coverage length is assumed to be 0.25m. Considering a total span of 33 m 132 nozzle arrays are required. For the spray cooling with vaporization of liquid water it was assumed that the same amount of water is required than for the vaporization or convective cooling. The pressure gas for the spray was not considered within the first estimation. A filter unit is required due to the risk of nozzle blockage.

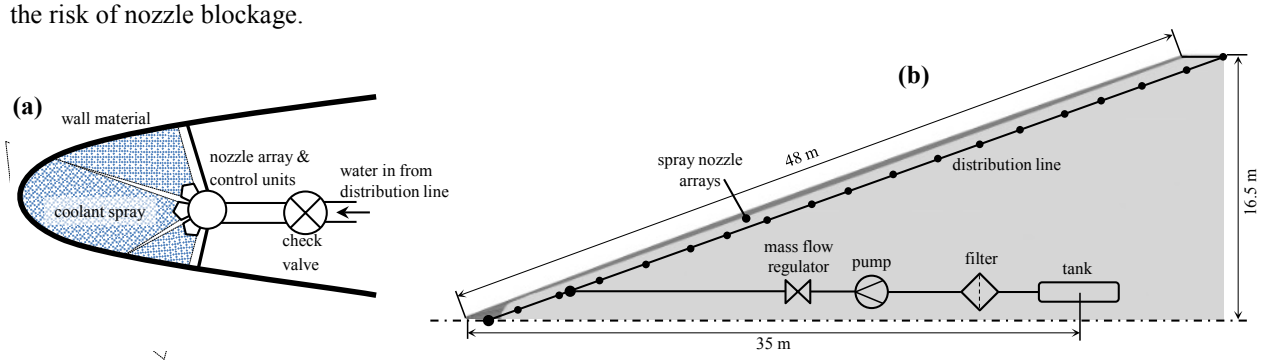

Figure 22. Potential preliminary design of spray cooling system for the SpaceLiner nose and leading edge, profile cross section (a) and plan view (b).

component	m [kg] (T_{obj}=500K)	m [kg] (T_{obj}=1000K)	m [kg] (T_{obj}=1500K)
pipes	146	146	146
tanks	320	295	241
filters	12	12	12
pumps	310	280	212
cooling unit	554	554	554
mass flow regulators	10	10	10
coolant	14890	13274	9791
total	**16242 (10.2%)**	**14571 (9.1%)**	**10966(6.9%)**

Table 5. Preliminary mass break down for the spray cooling system with liquid water.

As the presented results are based on very preliminary assumptions and engineering approaches more detailed analyses and designs will be necessary in the future.

D. Heat Conductive Fibers

In a theoretical investigation the potential increase in thermal conductivity of the C/C-SiC using pitch based carbon fibers was analyzed. A thermal model of the CMC microstructure was developed and the properties were simulated with an engineering approach (Figure 23) as well as with a detailed FEM analysis (Figure 24). The predicted improvement in thermal conductivity (under the assumption of a temperature independence of the fiber thermal conductivity) was an increase from 15-20 W/(mK) for standard PAN based fibers to 200-250 W/(mK) using pitch based fibers with a conductivity of 600 W/(mK). A summary of the in-plane and through the thickness (t-t-t) CMC thermal conductivity values calculated for different fiber thermal conductivities is given in (Figure 25).

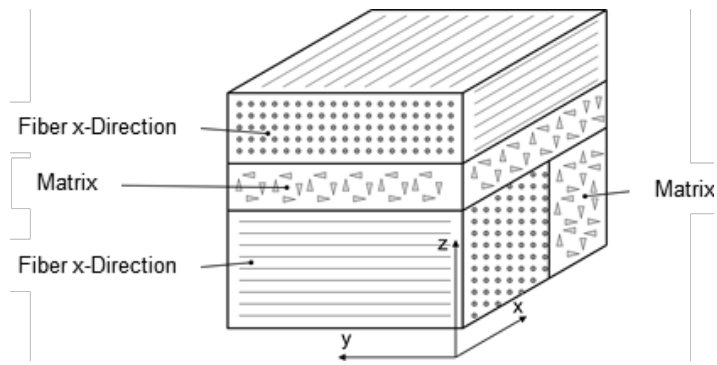

Figure 23. Block circuit model of a C/C-SiC ceramic matrix composite.

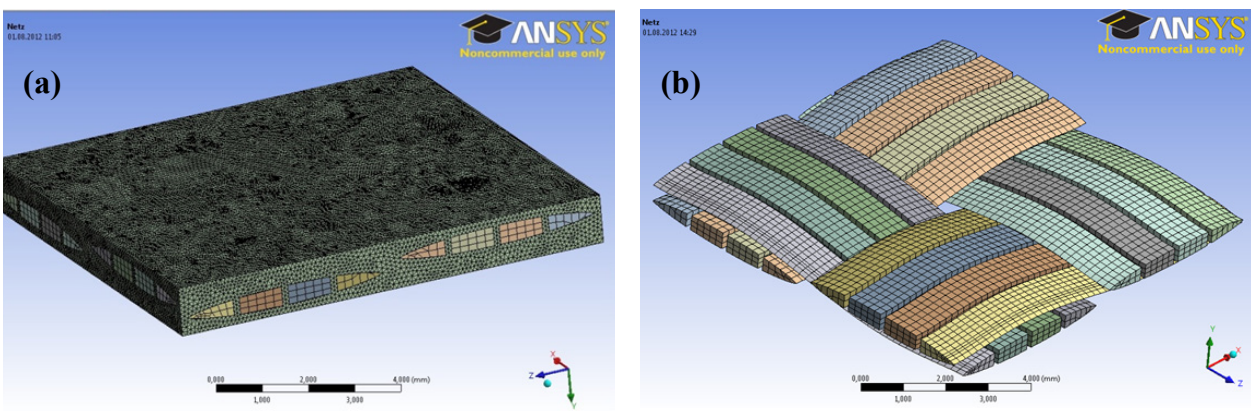

Figure 24. Finite element model of a C/C-SiC ceramic matrix composite w (a) and w/o matrix (b).

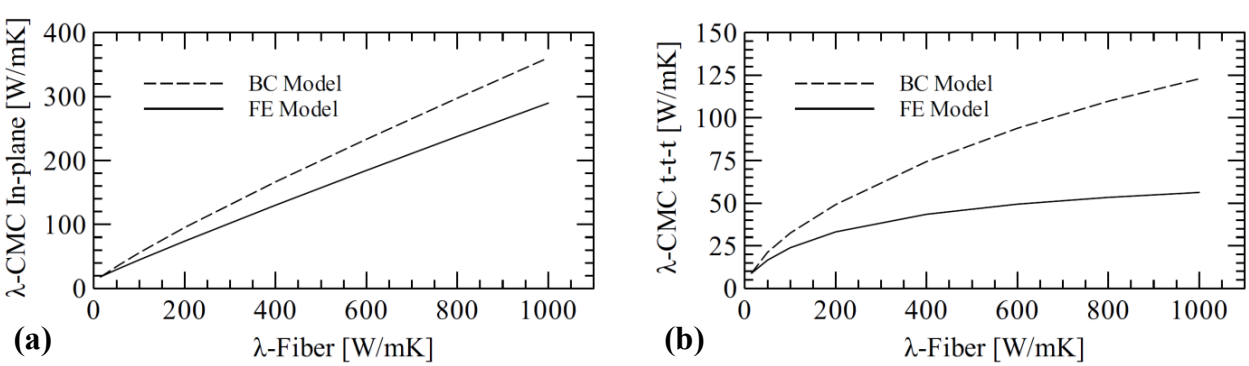

Figure 25. Simulated CMC thermal conductivity via block circuit and finite element model, in plane (a) and through the thickness (b).

In order to better evaluate the effects caused by the thermal conductivity of the CMC a FE parametric study of an exemplary hypersonic leading edge was carried out. The geometry used is a 2D airfoil section with a nose radius of 35 mm and a skin thickness of 10 mm. Since the primary interest of this investigation concentrates on the strong

heat flux gradients of the leading edge region, only the first 1m of the airfoil having a chord length of 27.5 m was considered (Figure 26).

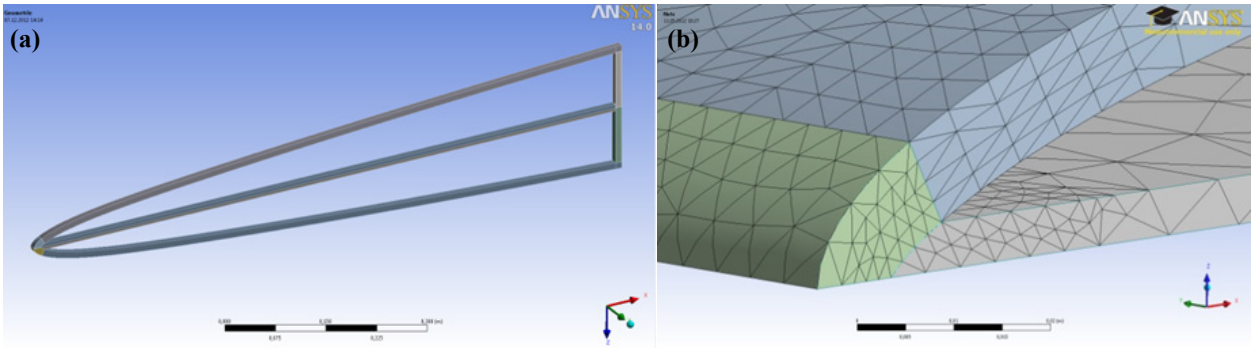

Figure 26. CAD Model of the leading edge and the generated FE mesh.

The heat transfer mechanisms implemented in the simulation are the heat transport inwards perpendicular to the wall, heat radiation outwards, internal heat radiation cavity. The leading edge was constructed in such a way that the heat bridge and the variation of the fiber orientation at the stagnation point region could be switched on or off. The considered simulation types A2 – A5 are summarized in Table 6.

parameter	simulation type			
	A2	A3	A4	A5
heat radiation outwards	x	x	x	x
heat transport inwards	x	x	x	x
internal heat radiation cavity	x	x	x	x
additional internal heat conducting structures (heat bridge)		x		x
adaptation of the fiber orientation at the stagnation point			x	x

Table 6. Summary of the simulation types A2 - A5.

A representative example of the results of the FE-study parameters, presented in Table 7 and Figure 27 is the case at Mach 10 with a thermal conductivity of the pitch based fiber of 1000 W/(mK). The introduction of a heat bridge and the adaptation of the fiber orientation at the tip show as expected a temperature reduction effect. The stagnation point temperatures for λ_{Fiber} of 15 and 1000 W/(mK) are summarized in the table below. Due to the geometric variations, that is, the introduction of a heat bridge and alignment of the fiber orientation at the tip a temperature reduction in the range of 20 to 65°C is achieved.

Mach 10	$T_{SP(\lambda Fiber=15\ W/mK)}$	$T_{SP(\lambda Fiber=1000\ W/mK)}$
(A2) no heat bridge	1867°C	1572°C
(A3) with heat bridge	1865°C	1541°C
(A4) no heat bridge with adaptation of the fiber orientation at SP	1851°C	1544°C
(A5) with heat bridge with adaptation of the fiber orientation at SP	1848°C	1505°C

Table 7. Stagnation point temperatures for the simulation types A2 to A5 at M=10; λ_{Fiber}=15-1000 W/(mK).

A significantly greater temperature reduction arises when the structure is made out of highly conductive material. The comparison between both fiber types gives a temperature reduction of 300 to 340°C. Thus a total temperature reduction of 360°C can be reached.

Following was the preparation and thermo-mechanical characterization of pitch carbon based C/C-SiC samples and comparison between the measured and simulated properties. Two fibers with a thermal conductivity of 220 W/(mK) and 600 W/(mK) respectively were selected for the study. The thermal diffusivity, specific heat capacity and density of the CMC were measured and its thermal conductivity calculated. Bending tests were also carried out and the fracture behavior of the material was evaluated. The results show an increase in thermal conductivity of the CMC by roughly one order of magnitude [at RT] when compared to standard PAN based C/C-SiC. The achieved conductivity values were ca. 100 W/(mK) [at RT] using a pitch based carbon fiber of 220 W/(mK) and ca. 150 W/(mK) [at RT] using a pitch based carbon fiber of 600 W/(mK). The temperature dependent thermal conductivities of the tested samples are shown in Figure 28.

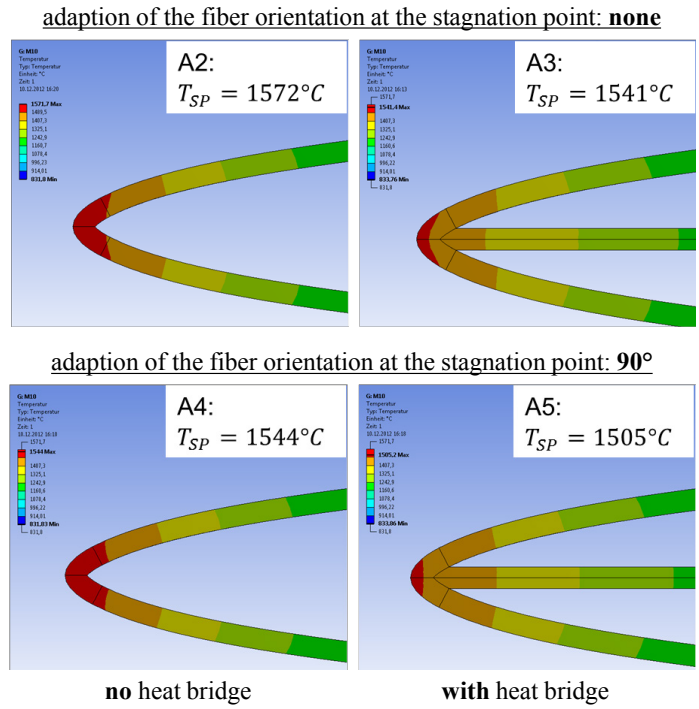

Figure 27. Results of the FE parameter study for the case: M=10; λ_{Fiber}=1000 W/(mK).

Subsequent manufacturing trials of larger material pieces in the form of flat plates were conducted. These were tested in the arc-heated wind tunnel L3K at the German Aerospace Center DLR in Cologne. The heating rate (time dependent thermal response) was measured with an infrared camera, thermocouples and pyrometers. The experimental results show the influence of the higher material conductivity and the effects of cavity radiation cooling. The results were compared to reference PAN fiber based C/C-SiC plate.

Arc-heated wind tunnel tests are planned for the evaluation of this highly conductive CMC in the form of angled plates having different nose radii. Thus the thermal response of the test structure to stronger heat flux gradients will also be analyzed.

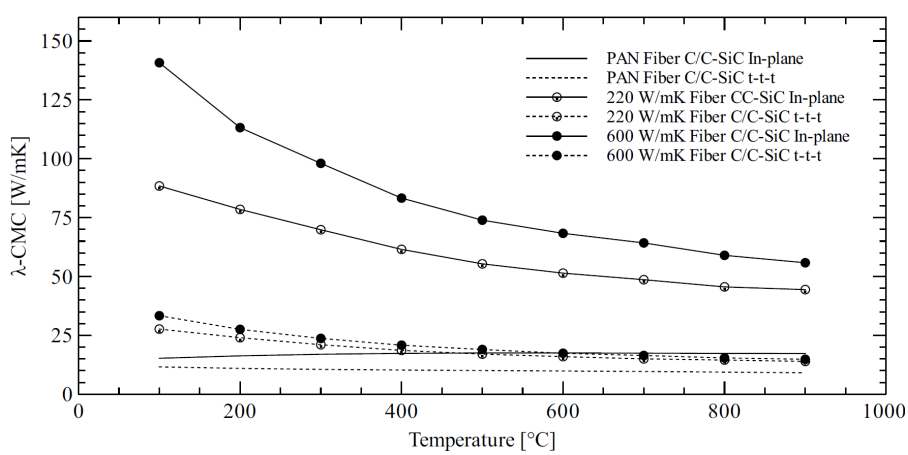

Figure 28. Temperature dependent thermal conductivity of C/C-SiC test samples made from pitch based carbon fibers and PAN based carbon fibers respectively.

VI. Conclusion

Potential active thermal protection systems were studied for the stagnation regions of the SpaceLiner reference vehicle. The specifications and requirements of the SpaceLiner mission were defined and a literature research was conducted in order to identify the most promising approaches for system architectures and coolants and to detect potential issues and problems related to the specific approach. Based on the literature research three different cooling systems were analyzed on a preliminary systems level for the SpaceLiner, transpiration cooling, convective cooling and spray cooling. Furthermore in the framework of the THERMAS project, a passive method of heat transport with highly conductive fibers was investigated. Preliminary mass estimations were performed. As a result it can be stated, that the coolant mass is the main impact factor on the total systems mass. Therefore hydrogen is preferable because of its very low mass, its availability due to the propulsion system and it very high specific heat capacity. However, hydrogen is highly flammable and safety issues must be considered. For transpiration cooling hydrogen is not suitable for that reason. Liquid water is also an efficient coolant due to its high vaporization enthalpy. The problems concerning water are mainly related to control issues and two-phase flows, which are complicated to manage. In terms of system architecture it can be stated, that the internal cooling systems are preferable because the ambient flow is not affected as for the transpiration cooling. In terms of accurate control of the coolant mass flows the spray cooling should be preferred. Based on the preliminary mass estimation, spray cooling is also the system with the lowest mass. However, more detailed studies and system designs will be necessary in the future to provide consistent approaches.

Acknowledgments

Part of this work was performed within the DLR research project THERMAS. THERMAS focuses on the development and demonstration of novel hybrid structures with integrated innovative thermal control elements.

Furthermore the authors gratefully acknowledge the contributions of Ms. Carola Bauer, Ms. Nicole Garbers, Mr. Ali Gülhan, and Mr. Dominik Neeb and all colleagues who are involved in the THERMAS project or in the preliminary design of the SpaceLiner concept.

References

[1]Sippel, M., Klevanski, J., Steelant, J.: "Comparative Study on Options for High-Speed Intercontinental Passenger Transports: Air-Breathing- vs. Rocket-Propelled", IAC-05-D2.4.09, October 2005

[2]Sippel, M., Schwanekamp, T., Trivailo, O..: "Progress of SpaceLiner Rocket-Powered High-Speed Concept", IAC-13-D2.4.05, 64th International Astronautical Congress, Beijing, China, September 2013

[3]Reisch, U., Anseaume, Y.: "Validation of the Approximate Calculation Procedure HOTSOSE for Aerodynamic and Thermal Loads in Hypersonic Flow with Existing Experimental and Numerical Results", DLR research report, 98-23, 1998

[4]Streit, T., Martin, S., Eggers, T.: "Approximate Heat Transfer Methods for Hypersonic Flow in Comparison with Results Provided by Numerical Navier-Stokes Solution", DLR research report, 94-36, 1994

[5]Schwanekamp, T.: "Beschreibung des Netzgenerators GGH", DLR internal report, SART TN-008/2011, Bremen 2008

[6]Seider, D., Fischer, P. M., Litz, M., Schreiber, A., Gerndt, A.: "Open source software framework for applications in aeronautics and space", IEEE Aerospace Conference, Mountain View, March 2012

[7]Eldred, M. S. et. al.: "DAKOTA, a multilevel parallel object-oriented framework for design optimization, parameter estimation, uncertainty quantification, and sensitivity analysis: Version 5.4 User's Manual", Sandia National Laboratories, Albuquerque, December 2009

[8]Johnston, C. G., Gomez, A. V.: "Radiative, Ablative, and Active Cooling Thermal Protection Studies for the Leading Edge of a Fixed-Straight Wing Space Shuttle – Part V: Transpiration Cooled Heat Shields Performance", project technical report task E&DD-701A, 17618-H076-R0-00, NAS 9-8166, December 1970

[9]National Aeronautics and Space Administration: "Thermal Protection Systems", Report on the Aspects of Thermal Protection of Interest to NASA and the Related Materials R&D Requirements, Technical Memorandum X-650, February 1962

[10]Gomez, A., V.: "Radiative, Ablative, and Active Cooling Thermal Protection Studies for the Leading Edge of a Fixed-Straight Wing Space Shuttle, Part I: Analytical Methods", NAS 9-8166, December 1970

[11]Gomez, A., V., Curry, D., M., Johnston, C., G.: "Radiative, Ablative, and Active Cooling Thermal Protection Studies for the Leading Edge of a Fixed-Straight Wing Space Shuttle", AIAA Paper No. 71-445, AIAA 6th Thermophysics Conference, Tullahoma, Tennessee, April 1971

[12]van Foreest, A.: "Investigation on Transpiration Cooling Methods for the SpaceLiner", DLR-IB 647-2006/05, SART TN-004/2006, Cologne, Germany, 2006

[13]van Foreest, A. et al.: "Transpiration Cooling Using Liquid Water", Journal of Thermodynamics and Heat Transfer, Vol. 23, Number 4.

[14]Gülhan, A., Braun, S.: "An experimental study on the efficiency of transpiration cooling in laminar and turbulent hypersonic flows", Research Article, Springerlink.com, August 2010

[15]McConarthy, W., A., Anthony, F., M.: "Design and Evaluation of Active Cooling Systems for Mach 6 Cruise Vehicle Wings", NASA CR-1916, Washington D. C., December 1971

[16]Kelly, H., N., Blosser, M., L.: "Active Cooling From the Sixties to NASP", NASA Technical Memorandum 109079, Langley Research Center, Hampton, Virginia 236811-0001, July 1994

[17]Glass, D., E.: "Heat-Pipe-Cooled Leading Edges For Hypersonic Vehicle Airframes", MS 396, NASA Langley Research Center, Hampton, VA 23681

[18]Puschmann, F.: "Experimentelle Untersuchung der Spraykühlung zur Qualitätsverbesserung durch definierte Einstellung des Wärmeübergangs", Dissertation, Otto-von-Guericke-Universtiy Magdeburg, Germany, 2003

[19]Garbers, N.: "Latest Version of SpaceLiner´s TPS with TOP", DLR internal report, SART TN-026/2013, Bremen, Germany, 2013

[20]Meyer, F.: "Vorentwurfsuntersuchungen zur aktiven Kühlung thermisch hochbelasteter Regionen am Hyperschall-Passagiertransportkonzept SpaceLiner", DLR internal report, SART TN-007/2014, Bremen, Germany, 2014